Anomalous optical absorption in ultrathin Pb films

M. Jałochowski, M. Stróżak, and R. Zdyb
Institute of Physics, Maria Curie-Skłodowska University, Pl. M. Curie-Skłodowskiej 1, PL-20031 Lublin, Poland
(Received 24 January 2002; revised manuscript received 5 June 2002; published 27 November 2002)

Ultrathin Pb films on Si(111)-(6×6)-Au deposited at 100 K are investigated by scanning tunneling microscopy, reflection high energy electron diffraction, and optical reflectance methods. From the reflectance data for light with a photon energy from 0.5 to 3 eV, the imaginary part of the Pb dielectric function ε^{Pb} is determined. For films with a thickness of 12 ML, the Pb ε^{Pb} vs photon energy resembles that expected for a bulk material. At smaller coverages the absorption spectrum shows anomalous, sharp optical structures. These structures are identified as strongly enchanced optical transitions characteristic of bulk materials. Simultaneously, a reduction of the free-electron Drude absorption is observed. This phenomenon is explained in terms of reduced electron screening. Our findings supply evidence of a bulklike electron band structure in ultrathin films and nanoparticles of Pb deposited on Si(111)-(6×6)Au.

DOI: 10.1103/PhysRevB.66.205417 PACS number(s): 78.66.Bz, 73.20.−r, 68.55.−a

I. INTRODUCTION

Optical reflectance and absorption experiments are considered to be among the most direct techniques to study the bulk band structure. Particularly when applied to insulators and semiconductors, they can deliver detailed and valuable information. In the case of metals their usefulness is greatly reduced. For frequencies below the bulk plasma frequency the interband absorption is reduced in strength and becomes near featureless. First, an external electric field induces a collective motion of all electrons, which in turn may screen this field and reduce possible resonant transitions at this frequency. Second, a superposition of all possible transitions over the entire Brillouin zone (BZ) between electron states, usually formed by a complicated set of various dispersion curves, results in the appearance of broad and weakly developed absorption peaks. These interband peaks are superimposed on a strong and featureless spectrum of free electron plasma absorption. In addition, strong electron scattering smears all interband transitions and further broadens the observed features.

In ultrathin metallic films the quantum size effect (QSE) may appear. In the electron-in-a-box model the bulk electron-free band structure splits into electron-free subbands. Usually the motion of electrons in the direction of quantization and in the plane of the sample can be treated separately. This model was successfully used to explain QSE electron photoemission phenomena,[1] electrical resistivity oscillations,[2,3] and the electron tunneling into the QSE states in a Pb thin film.[4] Even self-organization phenomena, observed recently during Pb film growth, were explained by the QSE within the framework of the free-electron model.[5,6] But the model is not sufficient if a real band structure in both perpendicular and parallel directions plays an important role, and if a sample is extremely thin. This was clearly seen in Hall effect experiments[7] with ultrathin Pb films. The one-dimensional electron-free model predicts a negative Hall coefficient, whereas the observed cofficient is positive even for thick films. In addition, in ultrathin films, the model shows a strong thickness dependent oscillation and reverses its sign several times. Obviously, a more realistic band structure model has to be considered. Unfortunately, theoretical studies of optical properties of quantized ultrathin metallic films deal with simplified models based on the electron-free band structure.[8–10] Few known experimental works[11,12] confirmed theoretical predictions.

Even less is known about the electronic and optical properties of metallic dots. When species contain only a few atoms, interesting effects can be expected. With a reduction in size, apart from more a pronounced QSE, a diminishing of the collective excitations of electrons is also expected.[8] Finally, upon a further reduction of size, the atomic behavior of the species should emerge.

The aim of this work is to study optical properties of extremely thin Pb films which in other experiments show the clear QSE effects.[1–3,7] Particularly, we study samples with Pb coverages close to 1 ML, where a homogeneous layer splits into separated islands approaching quasi-zero-dimensional structures.

II. EXPERIMENT

Samples were prepared in a ultra high-vaccum (UHV) chamber equipped with a reflection high energy electron diffraction (RHEED) apparatus, and a gas-flow UHV liquid helium cryostat for cooling of the samples during film deposition and during optical measurements. The vacuum system was also furnished with a quartz film-thickness monitor and with low temperature scanning tunneling microscopy (STM) (type Omicron VT). The base pressure was 5×10^{-11} mbar. The Si samples used here with dimensions of $18\times5\times0.6$ mm^3 and with a 20 Ωcm specific resistivity at room temperature, were fabricated from a *p*-type boron-doped single-crystal. Flashing for a few seconds to about 1500 K resulted in removal of SiC and in appearance of the 7×7 superstructure RHEED pattern. Direct resistive heating was used. In order to produce a Si(111)-(6×6)Au reconstruction, about 1.2 ML of Au were deposited onto the Si(111)-(7×7) and annealed for 1 min at about 950 K, and then the temperature was gradually lowered to about 500 K within 3 min. The (6×6)-Au superstructure production process was controlled by RHEED and STM.

The differential reflectance spectroscopy technique consists of measurements of a relative change of a substrate reflectance upon thin film deposition, $\Delta R/R=(R^{Si+Pb}-R^{Si})/R^{Si}$, where R^{Si} and R^{Si+Pb} are the reflectance of a bare substrate and a substrate covered by a Pb deposit, respectively. The angle of incidence of light beam ϕ was equal to 58.5°. The apparatus consisted of a quartz halogen lamp, a prism monochromator, a polarizer, a PbS photoconductor for light energies below 1.2 eV, and a Si-photodiode above this energy. The temperature of the detectors was stabilized at $-10\,^{\circ}$C. The light beam was chopped with frequency equal to 73 Hz. A lock-in technique was employed to recover the signal. *s*- or *p*-polarized light entered the UHV chamber through a fused silica window and was focused on a sample. Convergence of the light beam at the sample was below 0.7°. The specularly reflected beam after passing second fused silica window was focused on the detector. The intensity of the reflected light was recorded during thin film deposition. The rate of Pb deposition was about one monoatomic layer of Pb(111) (ML) per min. Typically about 200 points of data were collected for each sample with the final thickness of about 4 nm. The whole optical setup was optimized in order to achieve a high stability of the signal and high accuracy of the measurements. The differential reflectivity (DR) data were recorded during the deposition of Pb as a function of thin film thickness *d* at fixed photon energies *E* within the range of $\hbar\omega=0.5$–3 eV. The DR curves for a particular thickness vs photon energy were calculated from the set of DR vs thickness experimental data. In this manner a high precision in detection of small variation of DR was achieved.

During the deposition of Pb the substrate was held at 100 K. The crystal structure of growing film was monitored with RHEED. RHEED oscillations were recorded simultaneously during optical reflectivity measurements, and were used for calibration of quartz crystal thickness monitor. The Pb samples for STM measurements were deposited on Si(111)-(6×6)Au substrates mounted on a cooled STM stage. The STM chamber was equipped with separate evaporators and a quartz crystal thickness monitor.

III. RESULTS AND DISCUSSION

A. Differential reflectivity

In a classic description a substrate and film immersed in a vacuum are characterized by local and isotropic dielectric functions $\varepsilon^{s}(\omega)$ and $\varepsilon^{f}(\omega)$, respectively. Applying the Fresnel laws derived from the Maxwell equations and continuity arguments, McIntyre and Aspnes[13] showed that when thickness of a film *d* is small with respect to the wavelength λ of incident light then for *p*-polarization the DR is

$$\frac{R_p^{Si+Pb}-R_p^{Si}}{R_p^{Si}}=\frac{8\pi d}{\lambda}\cos\phi \times \mathrm{Im}\left\{\frac{\varepsilon^{Pb}-\varepsilon^{Si}}{\varepsilon^{Si}-1}\,\frac{1-\dfrac{\varepsilon^{Pb}+\varepsilon^{Si}}{\varepsilon^{Pb}\varepsilon^{Si}}\sin^2\phi}{1-\dfrac{1+\varepsilon^{Si}}{\varepsilon^{Si}}\sin^2\phi}\right\}, \tag{1}$$

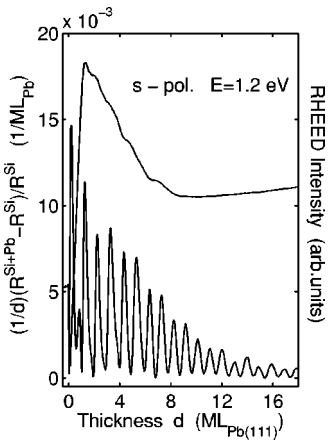

FIG. 1. An example of reflectance difference divided by the film thickness *d* measured *in situ*, during Pb deposition onto Si(111)-(6×6)Au at 100 K. The photon energy of *s*-polarized light was 1.2 eV. The bottom line shows RHEED intensity oscillations registered simultaneously with reflectance measurements.

with $\varepsilon^{Pb}=\varepsilon^{f}$ and $\varepsilon^{Si}=\varepsilon^{s}$. For *s* polarization the DR is

$$\frac{R_s^{Si+Pb}-R_s^{Si}}{R_s^{Si}}=\frac{8\pi d}{\lambda}\cos\phi\,\mathrm{Im}\left\{\frac{\varepsilon^{Pb}-\varepsilon^{Si}}{\varepsilon^{Si}-1}\right\}. \tag{2}$$

If the imaginary part of the dielectric function of the substrate is small then expressions (1) and (2) depend very weakly on the real part of thin film dielectric function. Thus, in order to extract the imaginary part of Pb thin film dielectric function, we can use the data for bulk Pb published by Lilienvall *et al.*[14]

Figure 1 shows an example of reflectance difference divided by the film thickness *d* measured *in situ*, during Pb evaporation onto Si(111)-(6×6)Au at 100 K. The photon energy of *s*-polarized light was 1.2 eV. From Eqs. (1) and (2) it follows that, for fixed energy, as long as optical constants are independent on thickness, the DR should increase linearly with thickness. Such a behavior is observed for thicker films, but for thinner films, below about 8 ML, a clear deviations from linearity is observed. Here visible dips with an approximately 2 ML periodicity can be correlated with similar specific resistivity variations measured previously.[2] Since the positions of dips are independent of the photon energy and the effect is much stronger at lower energies, we conclude that this modulation is closely linked with free electron excitation and, similar to the case of the electron resistivity phenomena, is caused by thickness dependent electron scattering of quantized conducting electrons. This figure also displays a simultaneously measured RHEED intensity variation. RHEED intensity oscillations clearly indicate a monolayer-by-monolayer growth mode from the very beginning of Pb deposition.

Figure 2 shows an imaginary part of the dielectric function of ultrathin films Pb $\mathrm{Im}(\varepsilon^{Pb})$ for selected thicknesses, derived from experimental data according to the Eq. (1) and divided by the wavelength λ expressed in μm, as a function of energy. This quantity is proportional to the absorption coefficient. Such a presentation also flattens the curve in the

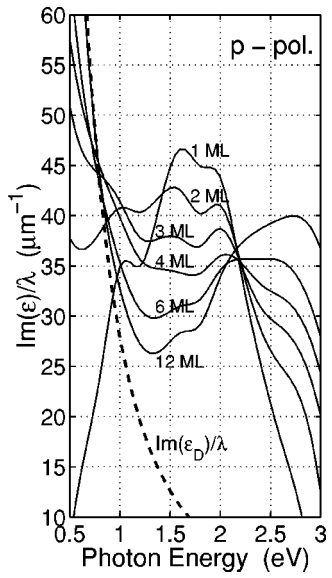

FIG. 2. Imaginary part of the dielectric function $\mathrm{Im}(\varepsilon^{Pb})$ divided by the light wavelength λ, derived from the experimental data for Pb films with coverages equal to 1, 2, 3, 4, 6, and 12 ML. Films are deposited on Si(111)-(6×6)Au at 100 K. $\mathrm{Im}(\varepsilon^{Pb})$ is calculated according to Eq. (1) for *p*-polarized light. The dotted line shows the free-electron (Drude) component of $\mathrm{Im}(\varepsilon^{Pb})/\lambda$.

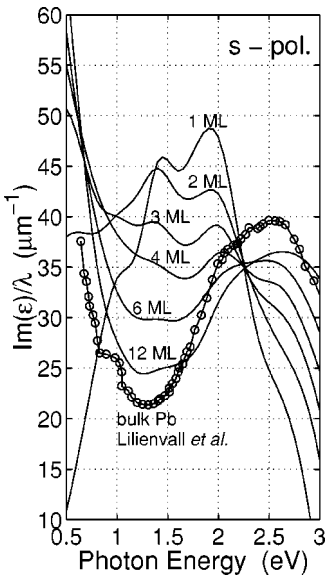

FIG. 3. Imaginary part of the dielectric function $\mathrm{Im}(\varepsilon^{Pb})$ divided by light wavelength λ derived from the experimental data for Pb films with coverages equal to 1, 2, 3, 4, 6, and 12 ML. Films are deposited on Si(111)-(6×6)Au at 100 K. $\mathrm{Im}(\varepsilon^{Pb})$ is calculated according to Eq. (2) for *s*-polarized light. The curve marked with empty dots is reproduced from Ref. 14.

low energy range where, due to the Drude absorption, a rapid increase of an imaginary part of the Pb dielectric function ε^{Pb} occurs. Here we also show a theoretical Drude component $\mathrm{Im}(\varepsilon_D)/\lambda$ of the dielectric function. For Pb the Fermi energy $E_F = 9.685$ eV, the Fermi wave vector $k_F = 15.96\ \mathrm{nm}^{-1}$, and the effective mass $m^* = 1.002 m_0$ (Ref. 1); the best fit to the low energy part of the curve for a 12-ML-thick sample was obtained with a mean free path *l* equal to 6.5 nm. At higher energies the visible difference between this theoretical curve and the experimental data for 12-ML-thick Pb is caused by the band structure features of bulk Pb. The presence of 1.2 ML of Au evaporated onto Si in order to induce a 6×6 superstructure was taken into account in calculations by utilizing an additive property of the differential reflectance.[15] The dielectric function of Au was taken from the work of Johnson and Christy.[16] Similar results were obtained from independent measurements for *s*-polarized light. Figure 3 shows $\mathrm{Im}(\varepsilon^{Pb})/\lambda$ evaluated from Eq. (2). For the sake of comparison the figure also presents results of Lilienvall *et al.*,[14] determined for a thick Pb film evaporated onto a fused quartz at room temperature.

Considering the band structure of bulk Pb, Liljenvall *et al.* identified broad absorption structures as being caused by interband transitions between approximately parallel bands around different points symmetry of the BZ. A peak close to 1 eV was identified at transitions around point *W*. A large absorption band extending from approximately 1.5 to 3.5 eV is believed to be caused by a superposition of interband transitions between parallel bands Σ_3 and Σ_1 and also between parallel bands along *W*-Γ. Generally, the main features of these experimental data were explained by energy band diagram obtained by Loucks,[17] but due to the broadening of the absorption peaks their precise identification and explanation is doubtful.

Our experimental data for a 12-ML-thick film of Pb, shown in Figs. 2 and 3, are similar to these of Liljenvall *et al.* Clearly, for this thickness, the optical constant approaches the bulk value. Dramatic changes occur in thinner films. With decreasing film thickness the absorption at 0.5–0.8 eV decreases drastically, whereas the absorption within the energy range from 0.8 to 2.2 eV increases. For the 1-ML-thick sample narrow peaks at about 1.0, 1.5, and 1.8 eV develop. A further reduction of the film thickness, below 1 ML, (Fig. 4), does not change the main features of absorption. The peaks become sharper, but their positions remain fixed.

B. Film morphology

For a proper discussion of optical properties at very low coverages a morphology of the Pb film has to be taken into account. Pb on Si(111)-(6×6)Au grew at 100 K in *monolayer-by-monolayer* fashion (the Frank–van der Merwe mode) as it was indicated by RHEED specular beam intensity oscillations. Our previous experiments[1–3,7] showed that such a growth mode in an early stage of deposition allows us to observe pronounced QSE. Films with coverages of less than 1 ML do not form continuous layer, and therefore need a more thorough discussion. Figure 5 shows a series of STM topographic images for clean Si(111)-(6×6)Au and Pb deposited on it with coverages 0.2, 0.65, and 1.05 ML. These samples were deposited and studied at 100 K. All images are presented with the same lateral scale. Also vertical magnification is the same for all samples. In Fig. 5(a) a well ordered Si(111)-(6×6)Au superstructure is visible. The surface roughness (rms) for this sample is equal to 0.018 nm. In Fig. 5(b) separate islands of Pb with the height roughly 0.2–0.3

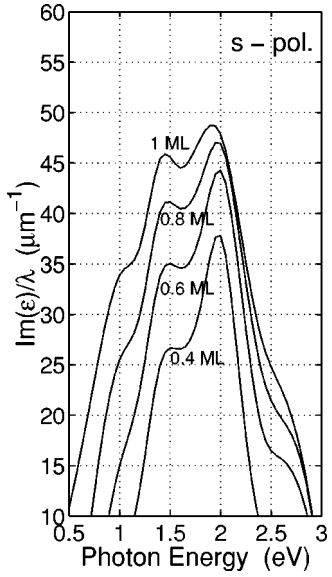

FIG. 4. Imaginary part of the dielectric function $\mathrm{Im}(\varepsilon^{Pb})$ divided by light wavelength λ derived from the experimental data for Pb coverages equal to 0.4, 0.6, 0.8, and 1.0 ML. Films are deposited on Si(111)-(6×6)Au at 100 K. $\mathrm{Im}(\varepsilon^{Pb})$ is calculated according to Eq. (2) for *s*-polarized light.

nm each containing of several Pb atoms are seen. There are other structures which in STM picture appear much smaller than these islands but larger than structures observed on clean Si(111)-(6×6)Au. We believe that these small features are produced by small nuclei containing a few atoms only. At a coverage of 0.65 ML the islands are larger, but still form a matrix of separate features. The size of these islands is about 1.5–2.0 nm, which corresponds well to the mean free path *l* of electrons in 5-ML-thick Pb at 70 K determined in electrical resistivity experiments,[3] equal to 2.0 nm. Figure 5(d) shows the surface of the sample with coverage of Pb slightly exceeding 1 ML. The surface roughness of this surface is larger than that of Si(111)-(6×6)Au, and the rms is equal to 0.030 nm. A presence of hills and grooves suggests that this 1.05-ML-thick film is composed of small domains with lateral size of about 1.5–2.0 nm.

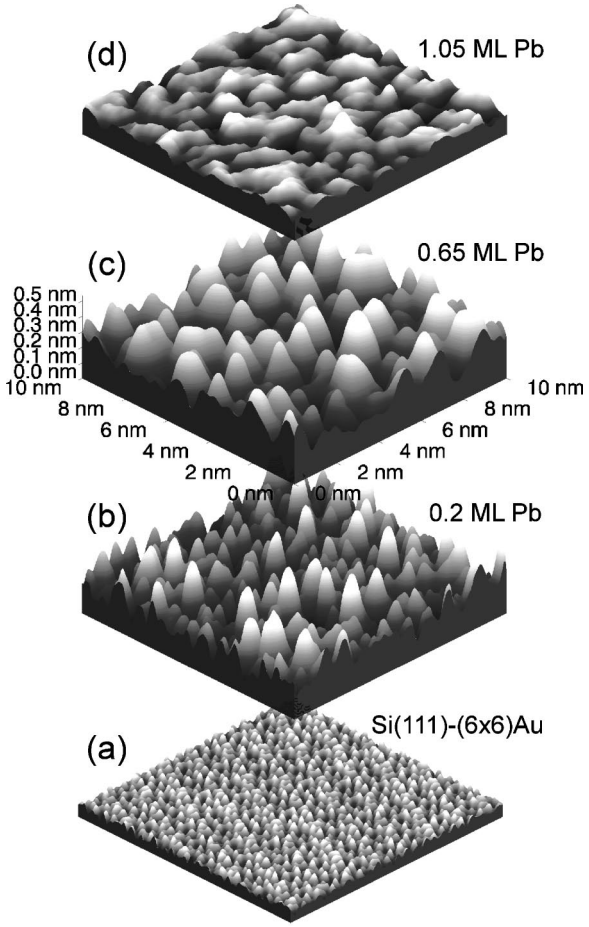

FIG. 5. STM topographic images for clean Si(111)-(6×6)Au (a), and Pb deposited on it with coverages 0.2, 0.65 and 1.05 ML [(b), (c), and (d), respectively]. All images are displayed in the same scale, with arbitrary vertical offset. In (b) separate islands of Pb with heights of roughly 0.2–0.3 nm, each containing several Pb atoms, are present. Their average diameter is about 1 nm. The average size of the islands increases with coverage and reaches about 1.5–2.0 nm at 0.65 ML of Pb in (c). In (d) the coverage of Pb slightly exceeds 1 ML. The presence of grooves suggests that the film is composed of small domains with a thickness equal to 1 ML and a lateral size of about 1.5–2.0 nm. The data were collected at sample biases equal to 0.31, -0.12, -1.44, and -0.096 V for (a), (b), (c), and (d), respectively.

IV. DISCUSSION

Surprisingly, well-resolved and strong absorption peaks of separate Pb islands, presented in Fig. 4, are almost at the same energies as in thicker films. In Fig. 2, the series of data for increasingly thicker films shows that positions of pronounced peaks at 1.0 and 1.5 eV remain constant. A peak at 1.8 eV shifts toward higher energies, and, finally, for thick films, forms a broad structure near 2.5 eV.

In order to explain experimentally determined optical properties of the thin Pb film, we turn to a bulk Pb band structure calculations. We assume that electronic states of Pb are described by the energy band model of Anderson and Gold[18] with four parameters: the Fermi energy, two pseudopotential coefficients, and a spin orbit coupling constant. Using their parameters we have performed band structure calculations in 1/24 of the irreducible Brillouin zone for a mesh of over 96 000 uniformly distributed triples of k_x, k_y, and k_z. The energies of these points were obtained as eigenvalues of the 8×8 complex matrix given by Anderson and Gold.[18] From these data the joint density of states (JDOS) was calculated. Results of the calculation are shown in Fig. 6. For the sake of comparison to the data presented in Figs. 2, 3, and 4, the JDOS data are multiplied by λ. This quantity, after the assumption of a constant matrix element for the optical transitions between two states, is proportional to the optical absorption. The presented curve possesses features showing similarities to the experimental data. As in the experiment the interband absorption begins at about 1 eV. At this energy a peak superimposed on the Drude absorption curve is visible. The second peak in Figs. 2, 3, and 4, located at about 1.5 eV, can be attributed to the rise of the JDOS at

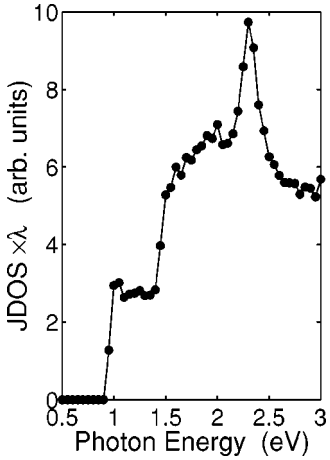

FIG. 6. Calculated joint density of states of bulk Pb multiplied by the wavelength of the light λ, as a function of the photon energy. This quantity is roughly proportional to the light absorption caused by interband transitions, and does not contain the absorption due to collective excitation, e.g., Drude absorption.

the same energy. We believe that the third peak in Fig. 4, located at about 1.9 eV for the 1-ML-thick sample, corresponds to the strongest feature in the JDOS, at about 2.3 eV. In the 12-ML-thick sample and in the data of Lilienvall *et al.*[14] it forms a broad peak centered at about 2.5 eV. As shown in Fig. 3, with increasing film thickness the peak shifts successively toward higher energies. Thus, qualitatively, the optical absorption of ultrathin films closely resembles the bulklike one. Moreover, the mezoscopic islands also show the same features as the continuous film.

The most striking feature of the experimental data is the emergence of narrow and strong absorption peaks at low coverages. The peaks are more pronounced for the lowest fractional coverages. In order to explain this behavior qualitatively we invoke the work of Silberberg and Sands.[9] They calculated the interband transition in a free-electron metallic quantum well perturbed by a collective electron motion of the electron plasma. Their main result was as follows. At high electron densities and below the plasma frequency, all the single electron transitions are, due to electron screening, either eliminated or greatly attenuated. Conversely, for low electron densities the screening has a negligible effect and single electron transitions (interband) dominate. As shown by Trivedi and Ashcroft,[19] in a very thin quantized metallic film a considerable lowering of the electron density is expected. According to their theory a 1-ML thick film of Pb, with only about 60% of the bulk value of the electron density, is expected. We conclude that the strong optical structures in 1-ML-thick film emerge due to a lowering of the electron screening. Also in small metallic particles the electron density, and thus also the electron plasma frequency, are strongly reduced due to QSE. This may even lead to a metal-insulator transition.[8] The reduced Drude absorption for the thinnest films in the low energy range strongly supports this assumption.

V. SUMMARY

In summary, we have shown that weak absorption features in the bulk material become more pronounced in the thinnest films. Surprisingly, even extremely thin films show interband optical transitions very similar to those of the bulk material. The strongest optical transitions are observed in the films composed of separated nanoparticles containing only a few atoms. The enhancement of the interband transition in ultrathin films and nanoparticles is attributed to reduced electron screening.

ACKNOWLEDGMENTS

This work was supported by Grant No. 7 T11B 049 20 of the Polish Committee of Scientific Research.

[1] M. Jałochowski, H. Knoppe, G. Lilienkamp, and E. Bauer, Phys. Rev. B **46**, 4693 (1992).
[2] M. Jałochowski, E. Bauer, H. Knoppe, and G. Lilienkamp, Phys. Rev. B **45**, 13 607 (1992).
[3] M. Jałochowski, M. Hoffmann, and E. Bauer, Phys. Rev. B **51**, 7231 (1995).
[4] I.B. Altfeder, K.A. Matveev, and D.M. Chen, Phys. Rev. Lett. **78**, 2815 (1997).
[5] V. Yeh, L. Berbil-Bautista, C.Z. Wang, K.M. Ho, and M.C. Tringides, Phys. Rev. Lett. **85**, 5158 (2000).
[6] M. Hupalo, V. Yeh, L. Berbil-Bautista, S. Kremmer, E. Abram, and M.C. Tringides, Phys. Rev. **64**, 155307 (2001).
[7] M. Jałochowski, M. Hoffmann, and E. Bauer, Phys. Rev. Lett. **76**, 4227 (1996).
[8] D.W. Wood and N.W. Ashcroft, Phys. Rev. B **25**, 6255 (1982).
[9] Y. Silberberg and T. Sands, IEEE J. Quantum Electron. **28**, 1663 (1992).
[10] O. Keller and A. Liu, Phys. Rev. **49**, 2072 (1994).
[11] J. Dryzek and A. Czapla, Phys. Rev. Lett. **58**, 721 (1987).
[12] Villagómez, O. Keller, and F. Pudonin, Phys. Lett. A **235**, 629 (1997).
[13] J.D.E. McIntyre and D.E. Aspnes, Surf. Sci. **24**, 417 (1971).
[14] H.G. Liljenvall, A.G. Mathewson, and H.P. Myers, Philos. Mag. **22**, 243 (1970).
[15] Y. Borensztein, T. Lopez-Rios, and G. Vuye, Phys. Rev. B **37**, 6235 (1988).
[16] P.B. Johnson and R.W. Christy, Phys. Rev. B **6**, 4370 (1972).
[17] T.L. Loucks, Phys. Rev. Lett. **14**, 1072 (1965).
[18] J.R. Anderson and A.V. Gold, Phys. Rev. **139**, A1459 (1965).
[19] N. Trivedi and N.W. Ashcroft, Phys. Rev. B **38**, 12 298 (1988).